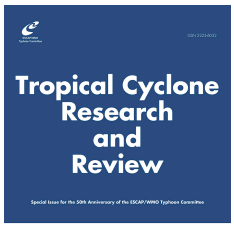

Advances in Tropical Cyclone Prediction on Subseasonal Time Scales during 2019–2022

Carl J. Schreck, III, Frédéric Vitart, Suzana J. Camargo, Joanne Camp, James Darlow, Russell Elsberry, Jon Gottschalck, Paul Gregory, Kurt Hansen, Justyn Jackson, Matthew Janiga, Philip J. Klotzbach, Chia-Ying Lee, Lindsey Long, Masuo Nakano, Kazuto Takemura, Yuhei Takaya, Michael J. Ventrice, Zhuo Wang

PII: S2225-6032(23)00025-5

DOI: https://doi.org/10.1016/j.tcrr.2023.06.004

Reference: TCRR 96

To appear in: *Tropical Cyclone Research and Review*

Please cite this article as: Schreck III., C.J., Vitart, F., Camargo, S.J., Camp, J., Darlow, J., Elsberry, R., Gottschalck, J., Gregory, P., Hansen, K., Jackson, J., Janiga, M., Klotzbach, P.J., Lee, C.-Y., Long, L., Nakano, M., Takemura, K., Takaya, Y., Ventrice, M.J., Wang, Z., Advances in Tropical Cyclone Prediction on Subseasonal Time Scales during 2019–2022, *Tropical Cyclone Research and Review*, https://doi.org/10.1016/j.tcrr.2023.06.004.

Advances in Tropical Cyclone Prediction on Subseasonal Time Scales during 2019–2022

Carl J. Schreck III[*1], Frédéric Vitart[2],
Suzana J. Camargo[3], Joanne Camp[4], James Darlow[5], Russell Elsberry[6],
Jon Gottschalck[7], Paul Gregory[4], Kurt Hansen[8], Justyn Jackson[9],
Matthew Janiga[10], Philip J. Klotzbach[11], Chia-Ying Lee[3],
Lindsey Long[7, 12], Masuo Nakano[13], Kazuto Takemura[14], Yuhei Takaya[15],
Michael J. Ventrice[16], Zhuo Wang[17]

[1]Cooperative Institute for Satellite Earth System Studies,
North Carolina State University, USA
[2] European Centre for Medium-Range Weather Forecasts, UK
[3] Lamont-Doherty Earth Observatory, Columbia University, USA
[4]Bureau of Meteorology, Australia
[5]Joint Typhoon Warning Center, USA
[6]Naval Postgraduate School, USA
[7]Climate Prediction Center, NOAA, USA
[8]National Research Council, USA
[9]U.S. Air Force, USA
[10]Naval Research Laboratory, USA
[11]Colorado State University, USA
[12]ERT, Inc., USA
[13]Japan Agency for Marine-Earth Science and Technology, Japan
[14]Climate Prediction Division, Japan Meteorological Agency, Japan
[15]Meteorological Research Institute, Japan Meteorological Agency, Japan
[16]DRW Holdings, USA
[17]University of Illinois at Urbana-Champaign, USA

[*] *Corresponding author*: Carl J. Schreck, III, E-mail: cjschrec@ncsu.edu

Abstract

This review describes advances in understanding and forecasting tropical cyclone (TC) subseasonal variability during the past four years. A large effort by the scientific community has been in understanding the sources of predictability at subseasonal timescales beyond the well-known modulation of TC activity by the Madden-Julian Oscillation (MJO). In particular, the strong modulation of TC activity over the western North Pacific by the Boreal Summer Intra-Seasonal Oscillation (BSISO) has been documented. Progress has also been realized in understanding the role of tropical-extratropical interactions in improving subseasonal forecasts. In addition, several recent publications have shown that extratropical wave breaking may have a role in the genesis and development of TCs. Analyses of multi-model ensemble data sets such as the Subseasonal to Seasonal (S2S) and Subseasonal Experiment (SubX) have shown that the skill of S2S models in predicting the genesis of TCs varies strongly among models and regions but is often tied to their ability to simulate the MJO and its impacts. The skill in select models has led to an increase over the past four years in the number of forecasting centers issuing subseasonal TC forecasts using various techniques (statistical, statistical-dynamical and dynamical). More extensive verification studies have been published over the last four years, but often only for the North Atlantic and eastern North Pacific.

Keywords: tropical cyclones, subseasonal, forecasts, hurricanes, MJO

1. Introduction

Camargo et al. (2019) reviewed the significant progress in our understanding and prediction of subseasonal tropical cyclone (TC) activity during 2015–2018. The current review provides a similar summary for the subsequent four years. A great advance in predicting subseasonal TC activity in the last four years has been the maturation of the Subseasonal Experiment (SubX; Pegion et al. 2019) and the World Meteorological Organization (WMO) Subseasonal-to-Seasonal (S2S; Vitart et al. 2017) model intercomparison projects. These models have produced increasingly skillful Madden–Julian Oscillation (MJO) forecasts beyond three weeks. Hybrid statistical–dynamical models have been created to leverage these MJO forecasts and the known relationships between the MJO and TC activity (e.g., Hansen et al. 2022). Some dynamical models can even produce skillful forecasts of subseasonal TC activity with minimal post-processing (Camp et al. 2018). The increasing skill of these models has empowered several operational forecast centers to produce experimental and even operational TC forecasts for week 3 (see section 4).

2. Modulation of TC activity by subseasonal modes of variability

2.1 Impact of tropical waves on tropical cyclone activity

In the four years since Camargo et al. (2019), many studies have focused on the sub-basin scale and elucidating how the MJO/Boreal Season Intraseasonal Oscillation (BSISO) modulates TC activity in tandem with other shorter period phenomena (e.g.,

tropical waves). Fowler and Pritchard (2020) showed that the South China Sea (100°E–120°E) is the most sensitive region in the western North Pacific (WNP) to the MJO/BSISO. In this region, the favorable decrease in vertical wind shear coincides with an increase in mid-level moisture. On the other hand, the eastern WNP (160°E-180°) is less sensitive to the MJO/BSISO because these factors are out of phase with one another: the increase in moisture precedes the decrease in vertical wind shear (Fig. 1). Along with the MJO/BSISO and the quasi-biweekly oscillation (QBWO), other modes of variability such as equatorial Rossby waves (ERW), Kelvin waves (KW), and the combination of Mixed Rossby-gravity waves (MRG) and tropical depression-type disturbances (collectively MRGTD) also contribute to TC genesis in the Bay of Bengal (BoB; Landu et al. 2020) and the WNP (Zhao et al. 2019). Landu et al. (2020) showed that during simultaneous ERW and MJO events, more TCs formed in the BoB than during any other combination of waves. ERW increased low-level vorticity, and the MJO increased moisture. On the other hand, simultaneous MRGTD and KW were associated with fewer BoB TCs than any other combination of waves. The MRGTD reduced vertical shear and contributed to drying at mid-levels, and KW decreased low-level vorticity, which results in fewer TCs in the BoB.

Understanding how TC tracks and thus landfall risk are modulated by the MJO/BSISO could potentially lead to better TC risk decision-making. In the WNP, TCs tend to move northwestward during the enhanced convective phases of the MJO/BSISO and QBWO, but during the suppressed convective phases recurving storms are more common (Wang et al. 2019; Ling et al. 2020; Nakano et al. 2021). A westward extension of the WNP subtropical high (Ling et al. 2020) or eastward extension of the monsoon

99 trough (Wang et al. 2019) lead to more northwestward-moving TCs during the
100 convective phases.

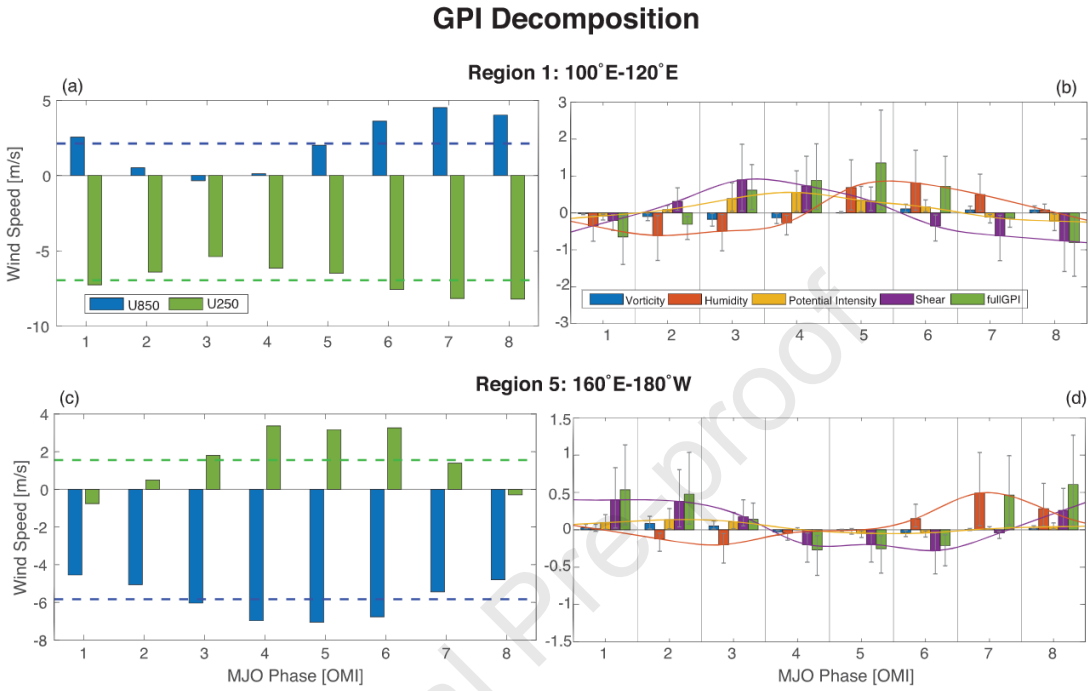

101

102

103 *Figure 1: (a, c) Average 850-hPa (blue) and 250-hPa (green) winds for each MJO*
104 *phase; dashed lines represent the Phase 1–8 mean. (b, d) Genesis Potential Index (GPI)*
105 *decomposition for each MJO phase, defined using the OLR-only MJO Index (OMI,*
106 *Kiladis et al., 2014). (from Fowler and Pritchard 2020)*

107 In addition to these sub-basin studies, significant progress has been made in
108 examining nonlinear interactions between the MJO and the El Niño Southern Oscillation
109 (ENSO). For example, Atlantic TC activity generally increases during La Niña episodes.
110 However, Hansen et al. (2020) found that the most favorable MJO phase for Atlantic TC
111 activity also shifts with the ENSO state. During neutral ENSO states, MJO phases 1 and
112 2 were associated with the highest level of TC activity in the Atlantic. During strong La
113 Niña states, MJO phases 4 and 5 were most likely to have above-average accumulated

cyclone energy (ACE; Bell et al. 2000). To investigate other potential factors that influence subseasonal TC activity, Hansen et al. (2020) developed a compositing technique that isolated subseasonal signals of environmental conditions in association with TC activity, which were referred to as ACE By Year (ABY). The most important predictors of enhanced TC activity were negative vertical wind shear anomalies in the North Atlantic Main Development Region (MDR), and positive vertical shear anomalies in the subtropical North Atlantic (Fig. 2). The vertical shear pattern associated with MJO phases 1 and 2 was similar to, but distinct from, the shear pattern in the ABY composite. Both nonlinear MJO/ENSO interactions and the subseasonal vertical shear signals appear to be linked to potential vorticity streamers, which suggests mid-latitude interactions may contribute to a significant portion of the subseasonal variability of North Atlantic TC activity (Hansen et al. 2020).

2.2. Impact of extratropical wave breaking on tropical cyclones

Several recent studies (Zhang et al. 2016, 2017; Li et al. 2018; Papin 2017; Papin et al. 2020; Jones et al. 2020) demonstrated that occurrence of extratropical Rossby wave breaking (RWB) events tend to reduce TC activity on subseasonal and longer time scales through larger vertical wind shear and mid-tropospheric dryness. Using semi-idealized numerical model simulations, Chang and Wang (2018) showed that these negative extratropical impacts on Atlantic TC activity may exceed the positive impacts of local sea-surface temperature (SST) anomalies in some years. Jones et al. (2022) showed that the dynamical impacts of RWB on vertical wind shear are predictable through the link between the North Atlantic Oscillation (NAO) and the RWB event. Thus, including such dynamical impacts may improve seasonal TC predictions. Zhang et al. (2021) analyzed a

large ensemble of climate simulations forced by observed SSTs and demonstrated that seasonal variations of RWB events are potentially predictable owing to SST forcing in both the tropics and extratropics.

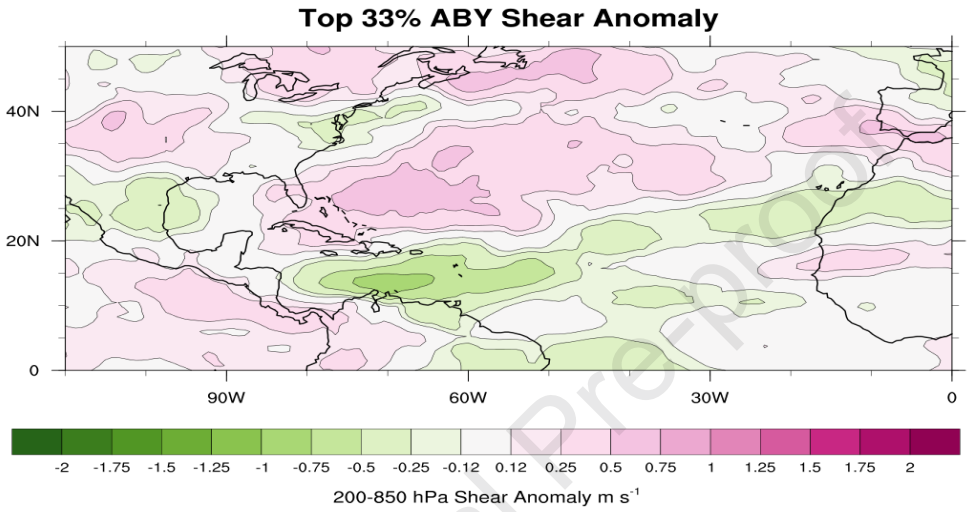

Figure 2: Vertical wind shear anomalies associated with subseasonal active TC periods in the North Atlantic using the ABY composite technique (from Hansen et al. 2020).

The tropical and extratropical impacts on TC activity can be integrated in the framework of summertime stationary waves. In particular, tropical upper-tropospheric troughs (TUTTs), interpreted here as stationary waves, are the preferred regions of RWB (e.g., Postel and Hitchman 1999), and become the regions of active interaction between the tropics and extratropics. These TUTTs are subject to the modulation by diabatic heating, which leads to variability of the North Pacific TUTT and the North Atlantic TUTT. This variability of large-scale environmental conditions thus contributes to the

150 variability of TC activity (Fig. 3). In addition, the anti-correlation of TUTTs between the
151 North Atlantic and North Pacific leads to the TC activities in the two basins tending to
152 compensate each other. Thus, the Northern Hemisphere TC activity may be less variable
153 than it would be if these two TUTTs were independent.
154

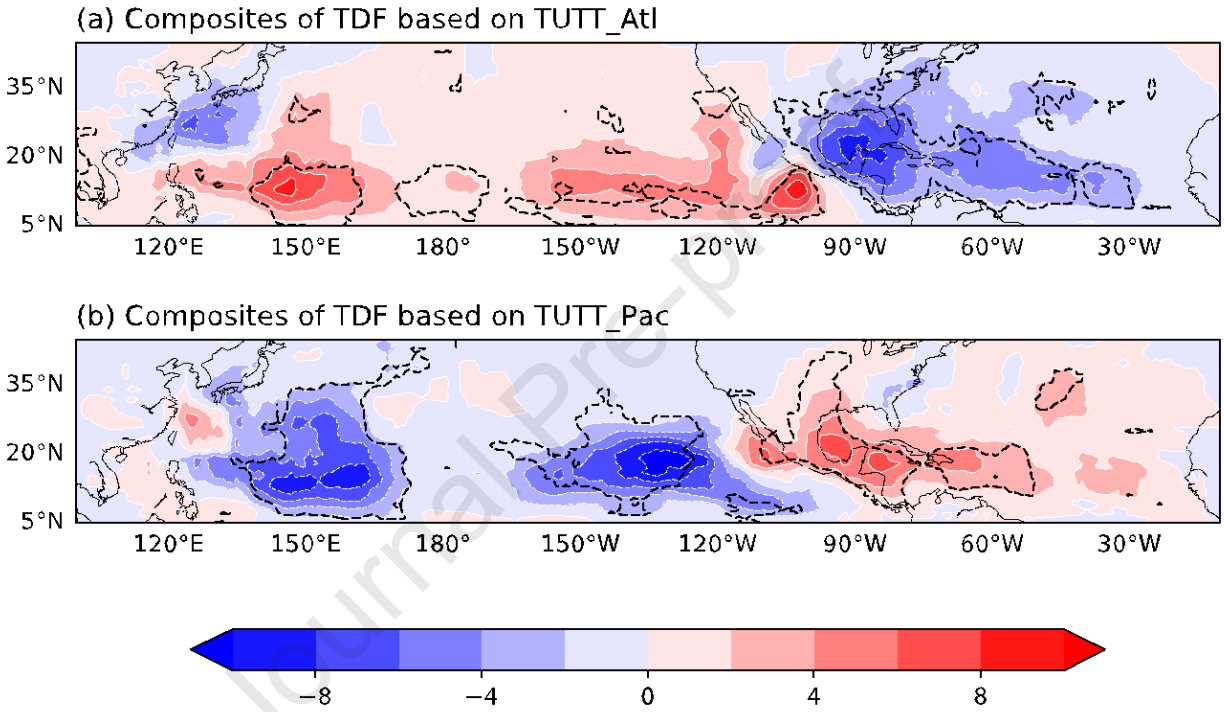

155

156 *Figure 3: Composites of tropical cyclone track density function (TDF, number of TCs per*
157 *month within a 10°×10° grid box) based on (a) the North Atlantic TUTT index and (b)*
158 *the North Pacific TUTT index. Dashed contours depict anomalies exceeding the 95%*
159 *confidence level. The TUTT index is defined based on the equatorward extension of*
160 *upper-level westerly flow over a subtropical ocean (adapted from Wang et al. 2020).*

161 While most recent studies have focused on RWB and North Atlantic TC activity,
162 Takemura and Mukougawa (2021) investigated tropical cyclogenesis over the WNP
163 triggered by RWB to the east of the Asian coast. A composite observational analysis
164 indicated that approximately 55% of the detected RWB events were accompanied by the
165 genesis and development of TCs to the southwest of the wave breaking center (Fig. 4). A

RWB event leads to an intrusion of the upper-level positive potential vorticity toward the southwest and consequently enhanced convection over the subtropical WNP. This enhanced convection is a favorable condition for TC genesis and development. It is noteworthy that Takemura and Mukougawa (2021) showed that no TC genesis occurred after the peak day of a RWB event.

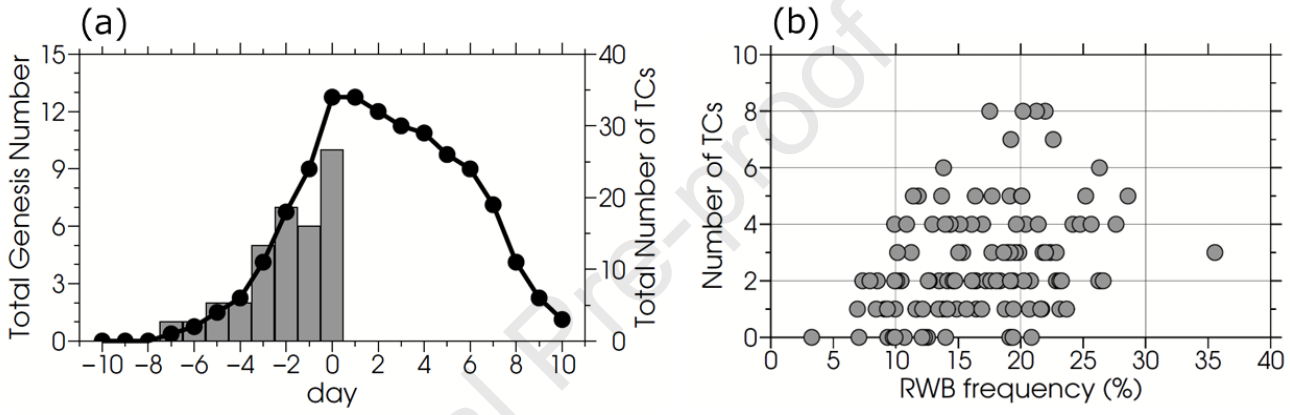

Figure 4: (a) Daily time series for the total numbers of TCs (black line; right axis) and TC genesis (gray bars; left axis) detected in 24 RWB cases during a period from 10 days before (day −10) to 10 days after (day +10) the peaks of RWB. (b) Scatter diagram between area-averaged monthly RWB frequency over 25°N–45°N, 140°E–180° and the monthly numbers of TCs detected from 15°N to 45°N and from 120°E to 180°E in July and August during the period from 1958 to 2018. (from Takemura and Mukougawa 2021).

3. Simulation of subseasonal TC activity in S2S and SubX models

3.1 Model description

Research on subseasonal-to-seasonal prediction of TCs has been accelerated by the maturation of multi-model datasets. There have been expansions and updates to the WMO S2S (Vitart et al. 2017) and the SubX (contains only North American models; Pegion et al. 2019) datasets. There are also new global model simulations and

187 improvements in global models that can potentially lead to advances in subseasonal TC
188 predictions. Some examples of these models are the GFDL SPEAR global coupled model
189 (Xiang et al. 2022a), the new version of the NASA GMAO GEOS S2S system (Molod et
190 al. 2020) and the Australia Bureau of Meteorology (BoM) ACCESS-S1 with an ensemble
191 Kalman filter (ACCESS-GE2, Gregory et al. 2020). Additionally, Richter et al. (2022)
192 showed that the CESM2 can be used as a community resource for research on
193 subseasonal predictability (see Table 1 for details).

194

195 *Table 1 List of available subseasonal TC reforecast datasets. V01 refers to the tracker*
196 *from Vitart and Stockdale (2001). Other than S2S TCs, data availability requires further*
197 *confirmation from each research group. (Table prepared by Dr. Jorge Garcia-Franco)*

Model	Native resolution	Coverage period (most updated)	Ensemble size	frequency	TC tracker	data availability
BoM	2°, L17	1981–2013	33	6/month	V01	S2S
CNRM	1.4°, L91	1993–2014	15	4/month	V01	S2S
CNR-ISAC	0.75°, L54	1981–2010	5	5 days	V01	S2S
CMA	0.5°, L56	2006–2020	4	2/week	V01	S2S
ECCC	0.35°, L45	1998–2017	4	weekly	V01	S2S
ECMWF	0.15°; 0.3° L137	2000–2020	11	2/week	V01	S2S
HMCR	1.2°, L28	1985–2010	10	weekly	V01	S2S
JMA	0.5°, L60	1981–2012	5	3/month	V01	S2S
KMA	0.75°, L85	1991–2016	3	4/month	V01	S2S
NCEP	1°, L64	1999–2010	4	daily	V01	S2S
UKMO	0.75°, L85	1993–2016	7	4/month	V01	S2S
CESM2 (CAM6)	1°, L32	1999–2020	11	weekly	Tempest Extremes	Climate Data Gateway
CESM2 (WACCM6)	1°, L70	1999–2020	5	weekly	N/A	N/A
GEOS-S2S-2	0.5°, L72	1999–2015	1	5 days	Tempest Extremes	Unk
SPEAR	0.5°, L33	2000–2019	10	5 days	Unk	Unk

198

Lee et al. (2020) evaluated regional TC events (genesis and subsequent track) in 20° longitude and 15° latitude boxes in the WMO S2S database models' reforecasts and found that the European Centre for Medium-range Weather Forecasts (ECMWF) model had one of the best performances in simulating the TC climatology as well as higher prediction skill. Lee et al. (2020) found that a key limitation in prediction skill of regional TC activity is genesis prediction, and the ECMWF model had the smallest errors in genesis climatology when compared to other WMO S2S models (Lee et al. 2018).

Camargo et al. (2021) reported that North Atlantic TC tracks in the ECMWF subseasonal reforecasts had clusters with similar characteristics to the observed. However, the ECMWF model had an additional cluster of recurving North Atlantic hurricane tracks near the coast of Africa with characteristics that do not correspond to the observed track clusters in that region, which may be due to some systematic biases in low-level winds and geopotential heights in the ECMWF model. When evaluating the climatology of TC intensity, model resolution was found to play an important role (Camargo et al. 2021; Gao et al. 2019). Gregory et al. (2020) compared subseasonal forecasts for the Southern Hemisphere among the ACCESS-S1, ACCESS-GE2, and ECMWF models and concluded that the superior performance of the ECMWF system was due to a larger ensemble size, higher spatial resolution, and an improved data assimilation scheme.

The MJO modulation of TC activity in these subseasonal forecast models has also been examined (Lee et al. 2020; Camargo et al. 2021). With the improvement of the MJO representation in models (Vitart 2017), the MJO–TC relationship is also simulated more realistically. Recently, Xiang et al. (2022b) suggested that landfalling TCs near the U.S.

222 coast can be influenced by three localized atmospheric circulation modes with significant
223 subseasonal (10–30 day) variability that is distinct from the MJO: (1) an anomalous low
224 pressure center in the eastern U.S.; (2) a zonal dipole pattern with a low pressure centered
225 in the western U.S. and a trough extending southeastward to the Gulf of Mexico; and (3)
226 a meridional dipole pattern with a low centered over the Caribbean Sea and a high over
227 central-eastern North America. There are more U.S. landfall TCs during the positive
228 phases of these modes. The GFDL SPEAR model can simulate these landfall track
229 modulations.

230 *3.2. Model verification*

231 Whereas the ECMWF model has the highest prediction skill among the WMO
232 S2S models (Lee et al. 2020; Fig. 5a), the skill analysis is sensitive to what validation
233 metrics are used as well as how the forecast is defined. Results from Lee et al. (2020) are
234 based on the verification of probabilistic predictions of regional TC activity measured by
235 the Brier Skill Score (BSS). When verified against a total seasonal climatological forecast
236 (BSS_c), reforecasts from ECMWF and Météo-France/Centre National de Recherche
237 Météorologiques models are skillful for most TC basins with lead times up to week 3 or
238 longer. The BoM model is skillful for Southern Hemisphere TC basins. However, when
239 validated versus weekly climatology activity (BSS_m), only the ECMWF model shows
240 skill in predicting TC occurrence anomalies beyond one week. In the Southern
241 Hemisphere, Gregory et al. (2020) showed that ACCESS-S1 is skillful in predicting TC
242 occurrence (not TC anomalies) at up to 3 week lead times. Regional BSS is not always
243 consistent with basin-wide mean BSS values, and the week 2 BSS for the ECMWF
244 system is shown in Fig. 5b.

In terms of TC ACE, the WMO S2S models have low prediction skill when measured by the Ranked Probability Skill Score (RPSS), which may be attributed to insufficient horizontal grid resolution to simulate either the TC's core structure or the occurrence of the most intense TCs (Lee et al. 2020; Camargo et al. 2021). Using the Heidke Skill Score (HSS) in reference to a random forecast, Gao et al. (2019) showed that the HiRAM model with a 8-km inner nested domain was skillful in predicting basin-wide (not regional) ACE associated with hurricanes and major hurricanes in the North Atlantic.

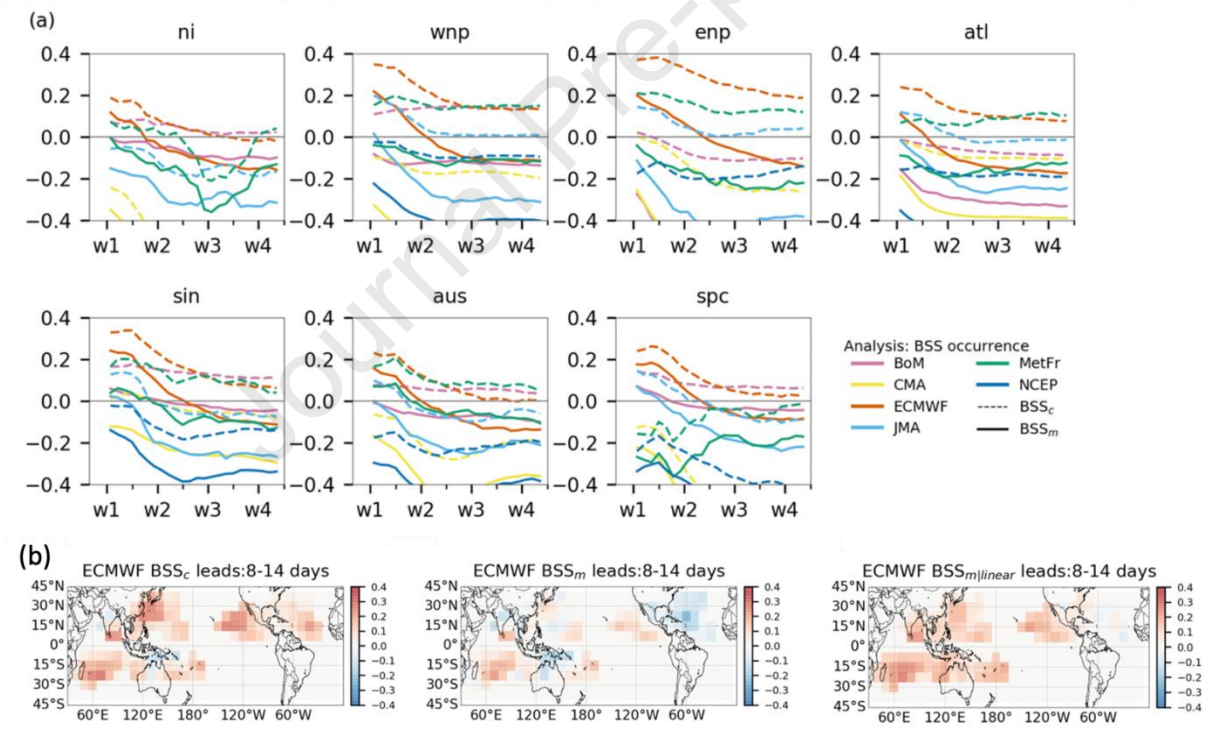

Figure 5: Brier Skill Score (BSS) of (a) regional TC occurrence predictions from six WMO S2S models, listed in the middle-row right and (b) global map of TC occurrence from the ECMWF model. BSS_c and BSS_m indicate seasonal-total and weekly-varying climatology references. $BSS_{m|linear}$ is the BSS_m for a bias-corrected forecast with a linear-regression bias-correction scheme. The TC basins are as follows: Atlantic (ATL), northern Indian Ocean (NI), western North Pacific (WNP), eastern North Pacific (ENP), southern Indian Ocean (SIN, 0°–90°E), Australia (AUS, 90°–160°E), and southern Pacific (SPC, east of 160°E) (from Lee et al., 2020).

Prediction skill of regional TC occurrence predictions can be improved via post-processing calibrations such as removing model mean biases (Camp et al. 2018; Gregory et al. 2020). Lee et al. (2020) showed that while removing mean biases works in some cases, it does not guarantee a positive impact globally. To improve a probabilistic forecast skill (often measured by BSS), one needs to increase the correlation between forecasts and observations and/or reduce the conditional and unconditional biases. Removing the mean TC occurrence biases reduces the unconditional bias to zero, but does not always guarantee a smaller conditional bias even in the training data. Thus, Lee et al. (2020) suggested a linear regression method (van den Dool et al. 2017) that removes the unconditional biases and minimizes the conditional biases. In addition, Gregory et al. (2020) showed that improved forecast skill could be obtained by using multi-model ensemble prediction, and including lag-averaged forecasts at t-12 h, t-24 h, etc. to increase the number of ensemble members.

Several recent case studies with deterministic or ensemble models have extended TC forecasts into the subseasonal TC range. For example, the landfall of Cyclone Hilda (2017) in northwestern Australia was predicted 2-3 weeks in advance by the ACCESS-S1 model, and the multi-model ensemble with the ACCESS-S1 and the ECMWF predicted cyclones Gebile and Gita (2018) two weeks in advance (Gregory et al. 2020). Domeisen et al. (2022) showed successful ECMWF ensemble week 3 or 4 forecasts for TCs Belna (2019, southern Indian Ocean), Claudia (2020, Australia), and Chan-Hom (2015, western North Pacific), which Domeisen et al. (2022) attributed to the occurrence of a strong MJO coinciding with the occurrence of these storms. This is consistent to findings from

Lee et al., which demonstrated that the WMO S2S models were more skillful when the convectively-enhanced phase of the MJO was active in that basin.

In addition to use direct TC forecasts from dynamic models, Kolstad (2021) suggested the inclusion of large-scale variables as predictors in a hybrid statistical–dynamical forecasting system could potentially extend the prediction time of potential precursor, and thus allow early detection of possible tropical cyclones. The hybrid model from Qian et al. (2020) indeed had superior forecast skills for predicting basin-wide tropical cyclone genesis count over the western-north Pacific, compared to the dynamical model that provided input to the hybrid model. Similarly, Maier-Gerber et al. demonstrated in 2021 that their hybrid model for subseasonal tropical cyclone activity in the North Atlantic Main Development Region and Gulf of Mexico had comparable skill to numerical weather prediction systems.

Lee et al. (2020) had earlier demonstrated that the WMO S2S models were more skillful when the convectively-enhanced phase of the MJO was active in that basin. However, the impact of the MJO on TC prediction skill varies by basin and by model. Kolstad (2021) recently suggested the inclusion of large-scale variables as predictors in a hybrid statistical–dynamical forecasting system could potentially extend the MJO subseasonal prediction time, and thus allow early detection of possible tropical cyclones. To that end, Maier-Gerber et al. (2021) showed that a hybrid model for subseasonal TC activity in the North Atlantic Main Development Region and Gulf of Mexico had comparable skill to numerical weather prediction systems.

4. Operational subseasonal forecasts of tropical cyclones

4.1. NOAA products

The NOAA Climate Prediction Center (CPC) provides the once-a-week Global Tropics Hazards (GTH) Outlook. An important component of informing the operational CPC GTH outlook is global TC identification and tracking utilizing S2S model data for the Weeks 1–4 target forecast period. The CFS, ECMWF, ECCC, and GEFSv12 operational ensemble model systems are utilized as forecast guidance for the GTH, and the TC activity is identified and tracked using the methods outlined in Camargo and Zebiak (2002). The forecasts are bias-corrected using a false alarm climatology based on model reforecasts and the National Hurricane Center (NHC) and the Joint Typhoon Warning Center (JTWC) best track datasets (Long et al. 2020). In addition to this model guidance, the GTH TC outlook includes (i) the state of ENSO and the MJO; (ii) coherent subseasonal tropical variability such as atmospheric KW, ERW, and African easterly waves (AEW); and (iii) interactions with the extratropical circulation (i.e., low-latitude fronts, wave breaking).

The Symmetric Extreme Dependency Score (SEDS)—a metric that focuses on relatively rare events—for TC tracks at Weeks 1–3 is shown in Fig. 6 for the CFS and ECMWF deterministic models, and for the GEFSv12 and the ECCC ensemble prediction systems for their respective reforecast periods. The contingency table for the SEDS calculations defines a hit when a forecastTC track point comes within a 3° box of a verifying TC track point within the same weekly interval. For clarity and to show better results, only the North Atlantic (ATL) and the eastern North Pacific (ENP) basins are shown. Note that the ENP has better skill than the ATL for both Week 2 and Week 3, and

329 the ECMWF has the best scores among the four models shown. Although forecast skill in
330 Week 3 is lower than in Week 2, it is noteworthy that substantial areas of skill have been
331 found for Week 3, and especially with all four models in the ENP basin.

332 *4.2. ECMWF forecasts*

333 ECMWF has issued week 1–4 forecasts of TC activity for each TC region since
334 2010 (Vitart et al. 2010). The TC forecast products include: (1) the predicted number of
335 tropical storms/hurricanes or ACE over a TC basin for a weekly period (calendar week 1–
336 4); and (2) a TC strike probability map: the probability of a tropical depression/
337 storm/intense storm (hurricane intensity) passing within 300 km (see example in Fig. 7).
338 Maps of TC strike probability anomaly relative to model climatology are also available.
339 These forecasts produced with the ECMWF TC tracker (Vitart and Stockdale, 2001) are
340 issued twice a week and are now publicly available. Tropical cyclone tracks predicted by
341 the ECMWF ensemble model during the 46-day integrations are available from the S2S
342 database, but with a 3-week delay (more information at www.s2sprediction.net). The
343 forecast skill of these forecasts has been evaluated in Camargo et al. (2021) for the North
344 Atlantic and by Lee et al. (2020) for the entire globe . It is planned in mid 2023 to
345 increase the frequency of these forecasts from twice weekly to daily and to increase the
346 ensemble size from 51 to 101 ensemble members. The objective is to provide more
347 frequent updates and more accurate probabilistic distribution functions of TC activity.

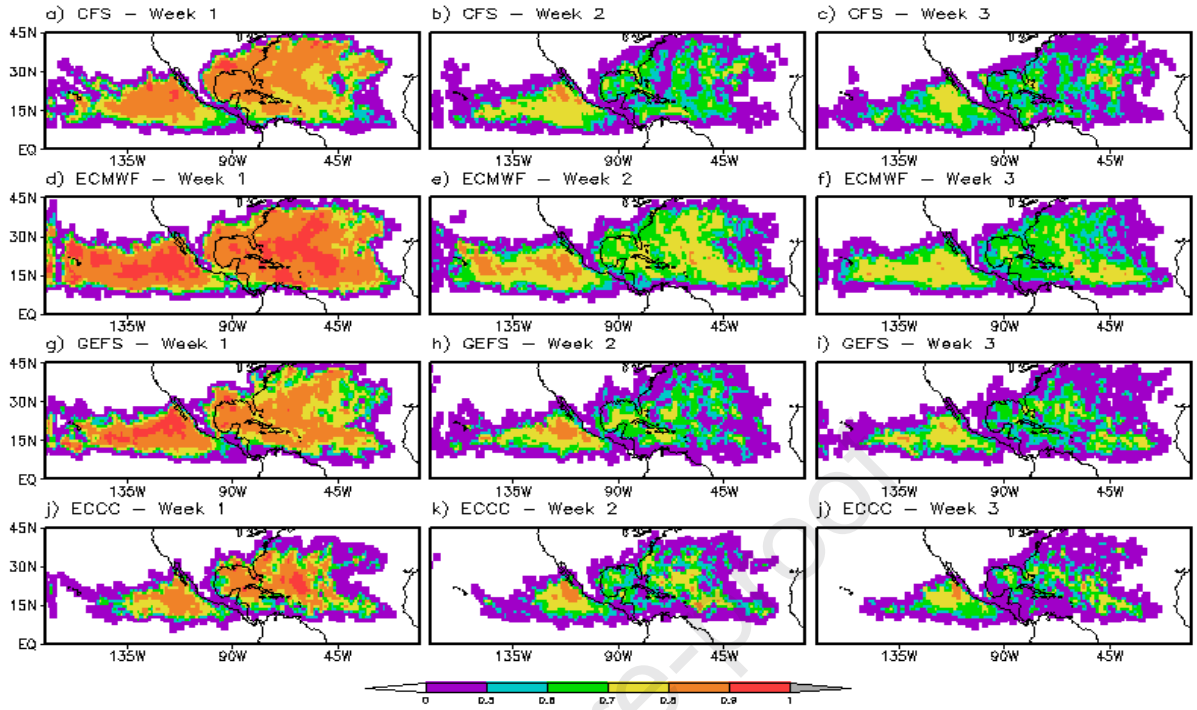

348

349 *Figure 6: Spatial maps of SEDS for TC tracks during Weeks 1-3 in the left, middle, and*
350 *right columns for the (a-c) CFS, (d-f) ECMWF, (g-i) GEFSv12 and (j-l) ECCC for the*
351 *ATL and ENP basins.*

352 The Elsberry et al. (2022) TC high-wind lifecycle guidance product based on the
353 ECMWF ensemble (ECEPS) could improve decision-making related to ENP TCs
354 compared to presently available probabilistic genesis or TC activity products. This
355 technique provides time-to-formation (T2F) and time-to-hurricane (T2H) to the nearest
356 six-hour synoptic time and at a position along generally highly accurate ECEPS track
357 forecasts of up to 15 days in length. In addition, the technique provides the ending time as
358 a hurricane (TEHU) and ending time as a tropical storm (TETS) along that up to the 15-
359 day ECEPS track forecast. For the first six hurricanes of the 2021 ENP season, the first

360 detections in the ECEPS were 8–12 days in advance of the T2F, and 9–13 days in
361 advance of the T2H.

362 A summary diagram is provided in Fig. 8 for both the pre-formation and the
363 ending of Hurricane Linda's track forecasts (panel b and panel a, respectively) and the
364 timing errors for these two variables (panels c and d, respectively). Whereas the first
365 NHC advisory forecast of pre-TS Linda was only 12 hours before the T2F in panel b, 19
366 ECEPS forecasts at 12-hour intervals were available prior to that T2F. Although there is
367 substantial track spread due to the variations in the initial positions, the cross-track spread
368 among these ECEPS forecasts that included both a TEHU and a TETS, the track spread
369 was reasonable considering that these forecasts started as early as 14 days before the
370 TEHU (panel b). The very small timing errors for the T2F and the T2H along these pre-
371 T2F tracks in panel (b) are presented in panel (c), and the generally small timing errors in
372 TEHU and TETS timing errors are presented in panel (d). This 15-day TC high-wind
373 guidance product in the ENP was in operational testing during the 2022 season and could
374 be extended longer in the subseasonal timeframe in the future if ECEPS forecasts are
375 extended.

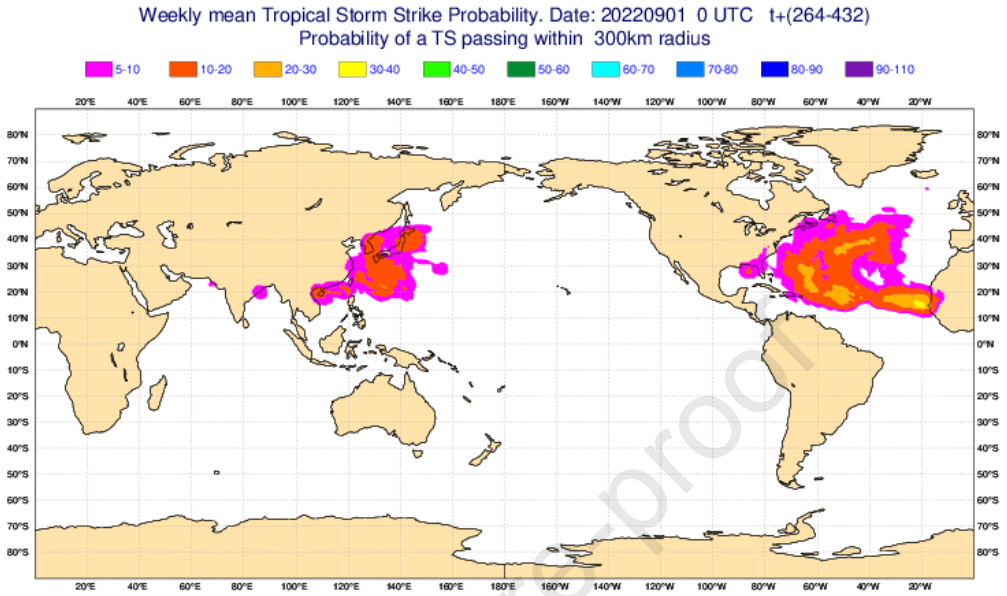

376

377 *Figure 7: Probability of a tropical storm strike within 300 km for the period 12 to 19*
378 *September 2022 from the ECMWF subseasonal forecast issued on 1 September (lead time*
379 *is day 12-18).*

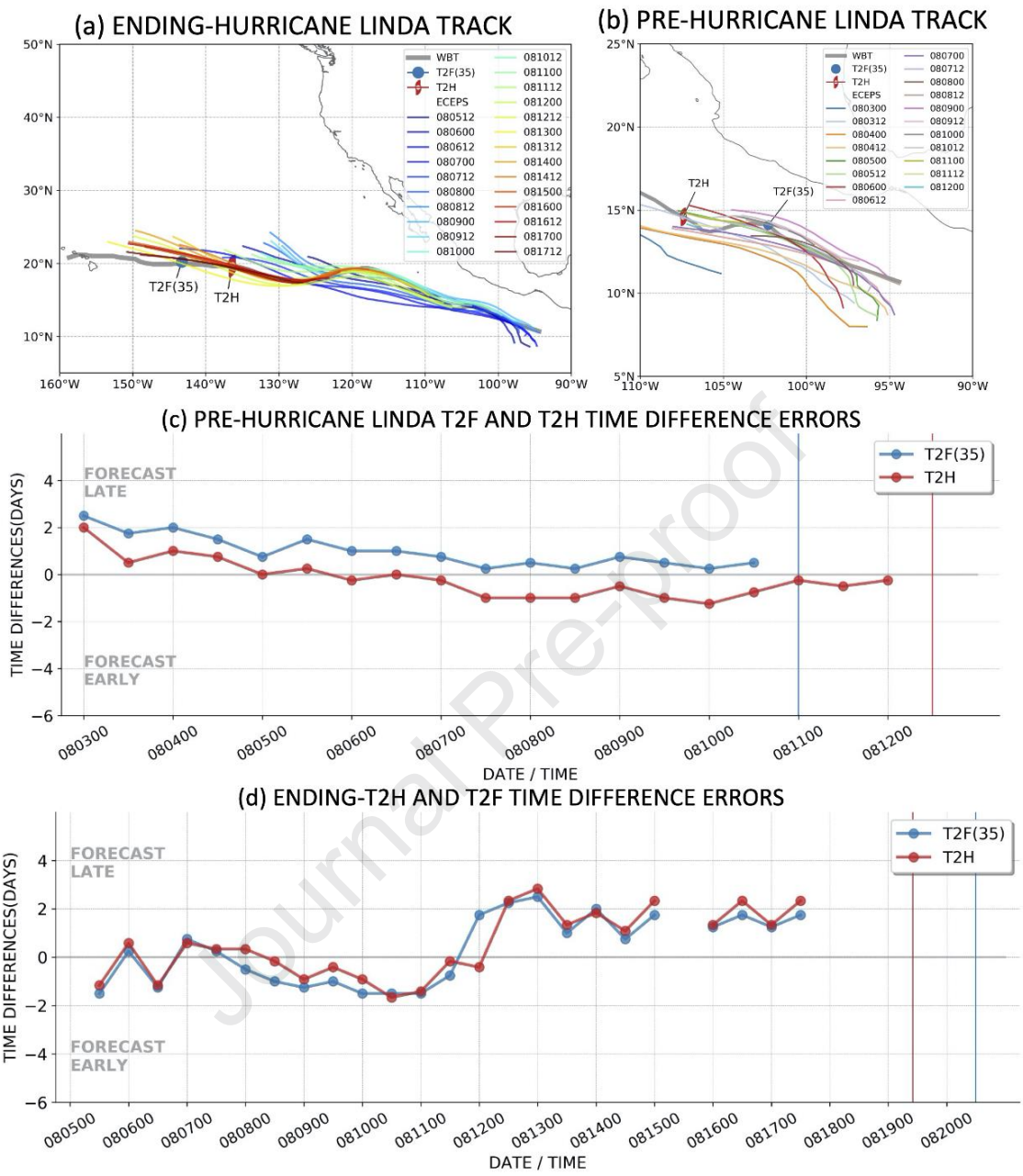

Figure 8: Summary of the ECEPS pre-formation and ending-stage predictions of the Hurricane Linda (2021) lifecycle. Track forecast initial times (MMDDHH) are indicated in the insets for the (a) ending stage and (b) pre-formation stage, and the T2F and T2H timing errors for the pre-formation and the ending-stage are displayed in panels (c) and (d). (from Elsberry et al. 2022)

387 *4.3. Australian Bureau of Meteorology forecasts*

388 The Bureau of Meteorology (BoM) makes available multi-week TC strike
389 probability forecasts for use by National Meteorological Services and the public (see
390 http://www.bom.gov.au/climate/pacific/outlooks/). Operational forecasts are currently
391 available for the South Pacific for weeks 2 and 3, and the WNP for weeks 2, 3 and 4.
392 Forecasts are updated daily during a region's TC season and a 2-week archive is also
393 made available. Three products are provided: (i) raw model probabilities of TC
394 occurrence; (ii) calibrated probabilities (following Camp et al 2018) and (iii) calibrated
395 probabilities relative to observed climatology.

396 Multi-week forecasts are produced using output from the ACCESS-S model,
397 which is based on the UKMO GloSea5 (MacLachlan et al. 2015). Version 1 of this
398 system (ACCESS-S1; Hudson et al. 2017) was operational during the period April 2018–
399 September 2021. This model showed impressive skill for predictions of the MJO out to a
400 lead time of ~30 days. These forecasts also showed skill over climatology for forecasts
401 of TC occurrence over the Southern Hemisphere for lead time weeks 1–5, when a spatial
402 and temporal calibration was applied (Camp et al. 2018). As indicated in section 3.2,
403 ACCESS-S1 provided useful guidance for the development of severe TCs, including
404 Cyclone Gita in the South Pacific and Cyclone Hilda off of the west coast of Australia, at
405 more than two weeks lead time (Gregory et al. 2019). Applying a wind speed threshold to
406 the model TCs also helped to reduce false alarm rates and improve forecast skill early on
407 in the forecast period (Gregory et al. 2019).

408 In 2020/21 ACCESS-S1 provided good guidance for severe TC Seroja, which
409 became the strongest TC to make landfall in southern Western Australia since 1956

(WMO, 2021). This cyclone presented a major challenge for forecasters due to its Fujiwhara interaction with TC Odette from April 7-9. A tropical low that failed to intensify was also in the region, moving south-east across the Cocos Islands from April 6-11. The uncertainty of the forecast was evident by the large spatial ensemble spread, and the associated low strike probabilities. Forecasts of the probability of TC occurrence for TC Seroja are shown for ACCESS-S1 for lead time weeks 2 and 3 in Fig. 9.

Following the successful trials for the Southern Hemisphere, research was extended to the WNP basin, and skill was found over climatology for calibrated forecasts of TC occurrence out to week 4 (BoM, 2020). Skill of real-time forecasts using a lagged ensemble of 2–3 days was found to provide increased skill for both the WNP and Southern Hemisphere for the trial 2017/18 and 2018/19 TC seasons (BoM, 2020). Finally, combining forecasts from the ECMWF's Medium- and Extended-Range Ensemble Integrated Forecasting System (IFS) and ACCESS-S1 to create a multi-model ensemble showed superior skill to the component models during the 2017/18 and 2018/19 TC seasons (Gregory et al. 2020).

In October 2021 the BoM operational system was upgraded to ACCESS-S2 (Wedd et al. 2022). This system retains the skill of the MJO out to ~30 days and shows skill over climatology for multi-week forecasts of TC frequency over the Southern Hemisphere, western and eastern North Pacific, and North Atlantic out to week 5. However, the skill over climatology in the North Indian Ocean was only to week 2 (Camp et al. 2023a,b).

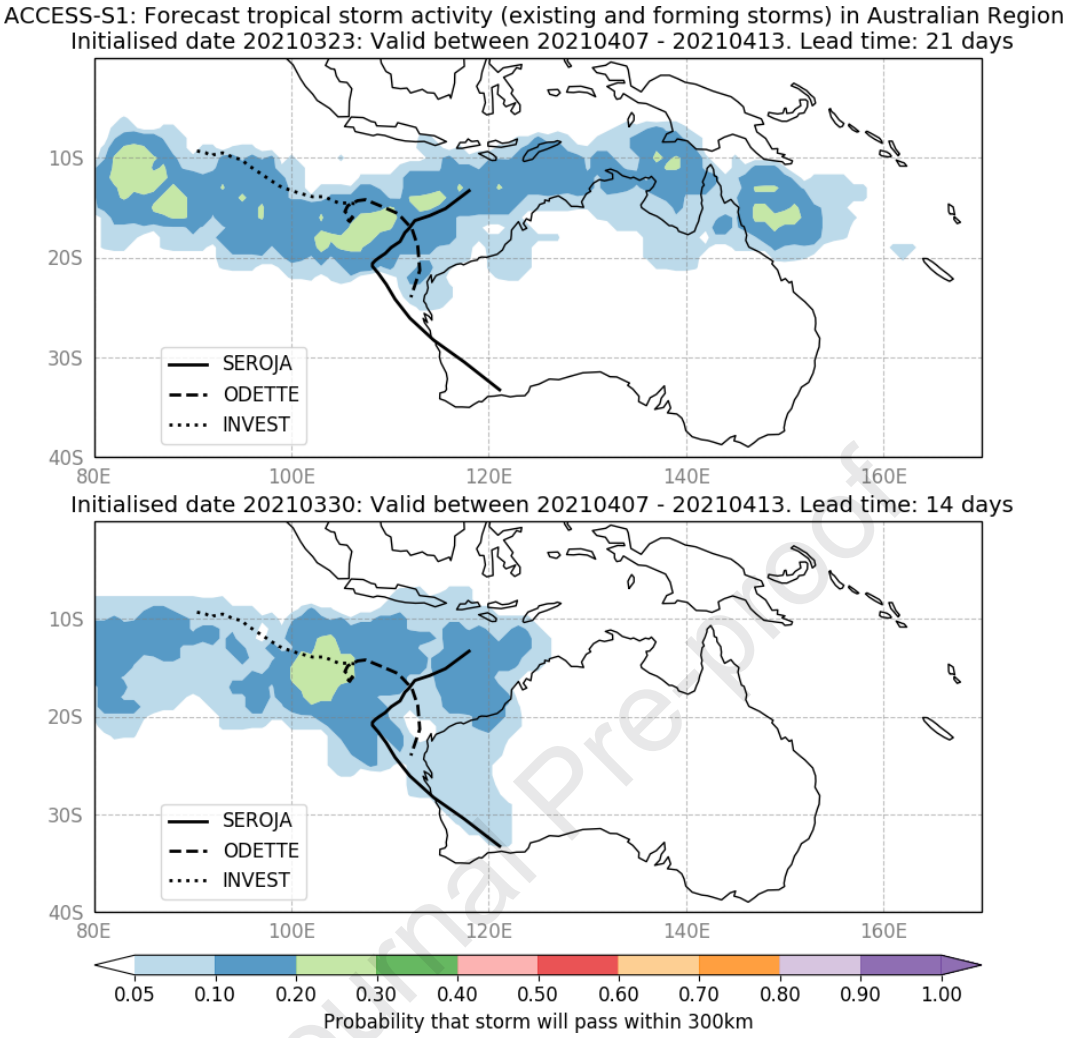

Figure 9: Probability of a TC passing within a 300 km radius for ACCESS-S1 forecasts valid in a) week 3 (initialized 23 March 2021) and b) week 2 (initialized 30 March 2021) for the period 7–13 April 2021. Corresponding observed tracks for TC Seroja, TC Odette and an invest area are overlain in black. Observed TC tracks are from the US Navy's Joint Typhoon Warning Center (JTWC; Chu et al 2002). TC Seroja made landfall on 11 April 2021.

4.4. Colorado State University forecasts

Colorado State University (CSU) has been operationally issuing two-week Atlantic basin ACE forecasts since 2009. These forecasts are issued six times during August–October. Each forecast is for the probability of above-normal, normal, or below-normal ACE terciles for the North Atlantic. These predictions are based on both

445 statistical and dynamical models and consider several different factors: (1) National
446 Hurricane Center (NHC) current and forecast North Atlantic activity; (2) NHC Tropical
447 Weather Outlooks; (3) Global model forecasts of North Atlantic TC development; (4)
448 Current and projected state of the MJO; (5) Global model forecasts of key atmospheric
449 circulation patterns; and (6) the current TC numbers relative to the CSU Atlantic seasonal
450 hurricane forecast.

451 For the sample of 78 two-week Atlantic TC forecasts since 2009, 64% have
452 verified in the correct tercile, 28% missed by only one tercile, and 8% missed by two
453 terciles. In general, these forecasts have shown improved skill in recent years, with only
454 one two tercile miss (e.g., forecast bust) since 2013.

455 *4.5. Joint Typhoon Warning Center*

456 In 2018, JTWC began providing graphical two-week TC Formation Outlooks that
457 depict geographic areas (boxes), timeframes, and forecaster-designated TC formation
458 probabilities in the Indian, WNP, and South Pacific basins. JTWC will continue to
459 generate and distribute these outlooks at least twice daily while exploring the viability of
460 longer period forecasts. For example, the JTWC and the 14th Weather Squadron (14 WS)
461 Climate Monitoring, Analysis and Prediction teams have conducted weekly collaboration
462 calls to coordinate 14 WS Week 3 TC formation outlooks for the JTWC forecast basins.
463 Although JTWC has no near-term plans to extend its two-week TC formation outlook to
464 the week 3 period, the collaboration has infused new tools and perspectives from 14 WS
465 climatology experts into the existing JTWC extended-range forecasting process.

466 The JTWC development efforts also benefit from extensive collaboration with the
467 NOAA CPC and U.S. Department of Defense (DOD) partner organizations. For example,

468 the 16th Weather Squadron (16 WS) numerical modeling team developed a suite of TC
469 prediction guidance for DOD forecasters. Included in the new 16 WS guidance is a multi-
470 model ensemble forecast of large-scale probability of wind speed exceedance that
471 effectively highlights geographic areas and timeframes in which TC formation may
472 occur.

473 *4.6. U.S. Naval Research Laboratory*

474 Hansen et al. (2022) examined whether nonlinear MJO/ENSO influences and the
475 subseasonal vertical shear pattern impacts on the North Atlantic ACE can be used to
476 improve subseasonal predictions. Hansen et al. built a statistical-dynamical hybrid model
477 using Navy-Earth System Prediction Capability (ESPC; Barton et al. 2020) reforecasts as
478 part of the SubX project (Pegion et al. 2019). Persistence reforecasts of Niño 3.4 SSTs
479 and MDR SSTs, and Navy-ESPC reforecasts of the first two principal components (PCs)
480 of the MJO, were used as predictors for the basic model. Two shear index predictors
481 evaluated from Navy-ESPC reforecasts were added in one option, and a second option
482 was substituting a nonlinear MJO/ENSO predictor in place of the MJO PCs and Niño 3.4
483 SST predictors. These predictors were fed into a logistic regression model, which adds
484 and removes predictors to assess the skill contribution from each predictor. The North
485 Atlantic SSTs and the MJO were found to be the most important factors contributing to
486 subseasonal North Atlantic TC activity (Fig. 10). The shear pattern improved forecast
487 skill at 5–10 day lead times before forecast shear errors became too large. Nonlinear
488 MJO/ENSO interactions did not improve skill compared to separate linear considerations
489 of these factors, but did improve the reliability of predictions for high-probability active
490 TC periods.

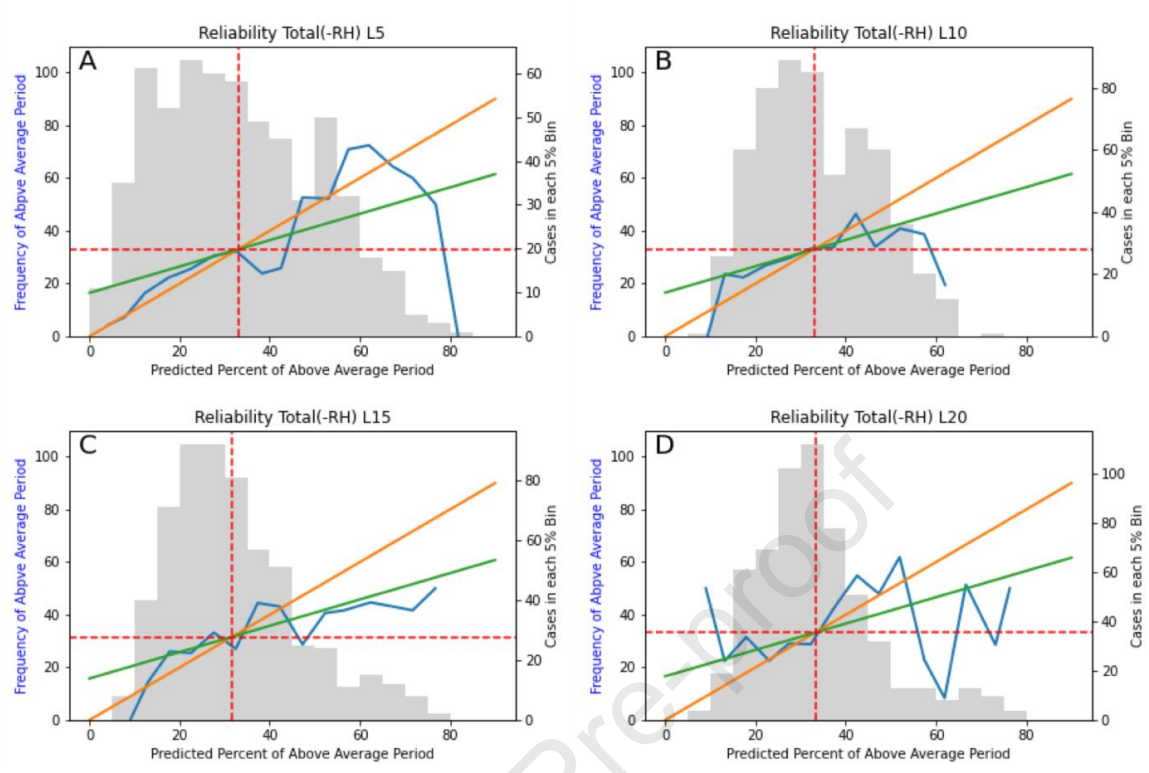

491

492 *Figure 10: Reliability diagrams for the "Total (-RH)" scheme, which includes the shear*
493 *predictors, MJO PCs, Nino 3.4 SSTs and MDR SSTs but not relative humidity (RH) for a)*
494 *5-day, b) 10-day, c) 15-day, and d) 20-day forecasts. The blue line indicates the observed*
495 *frequency of an above-average normalized 5-day ACE period for each 5% forecast bin.*
496 *The orange line indicates a one-to-one ratio of predicted probability and observed*
497 *frequency representing a perfect model. The green line indicates climatological skill.*
498 *Vertical and horizontal dashed red lines indicate the climatological rate of active*
499 *normalized 5-day ACE periods in the North Atlantic. Gray bars indicate the number of*
500 *forecasts that fall into each 5% bin. (from Hansen et al. 2022)*

501 *4.7. Private sector forecasts*

502 It is well known that a TC strike across an economic point of interest will drive a
503 chain of reactions across the global markets. These market reactions vary depending on
504 the intensity of the TC, the risk of inundation, and even the amount of rainfall.
505 Understanding these risks at longer lead times is always desired, which will require
506 improved numerical weather prediction (NWP) model forecasts of TCs at these long lead
507 times. At subseasonal forecast leads (i.e., forecast weeks 3+), private sector companies

508 often rely on a combination of NWP forecasts and tropical wave-based statistical
509 forecasts of TC activity. While there have been incremental advances in NWP forecasts
510 beyond 10 days, the prediction of TC impacts is still not reliable. This unreliability has
511 resulted in little to no advancements in subseasonal outlooks of TC impacts across the
512 private sector.

513 In recent years, there has been more desire to utilize the full distribution of an
514 NWP ensemble suite. As the private sector industry gains knowledge about medium-
515 range to subseasonal predictions of TCs, the community is shifting away from
516 deterministic NWP forecasts and toward probabilistic forecasts. Questions often asked by
517 decision makers are, "What is the range of outcomes that could happen?" or "What is the
518 probability of wind speeds greater than 100 mph across this specific location?" As
519 agencies continue to increase the number of ensemble members in their forecast models
520 and improve the forecast skill beyond 7+ days, more private sector groups rely on
521 ensemble probabilistic guidance to hedge risk in whatever TC decision they must make.

522 5. Summary and conclusions

523 Progress has been made by the scientific community over the last four years to
524 better understand the sources of predictability and the modulation of TC activity at
525 subseasonal timescales. In particular, several recent publications have evaluated the
526 impact of the BSISO on TC activity over the WNP. There has also been significant
527 progress in the understanding of the impact of extratropical wave breaking on tropical
528 storm development.

529 The availability of large datasets of subseasonal forecasts (S2S and SubX) has
530 been an opportunity to better understand the capability of S2S models to simulate and

predict the subseasonal variability of TCs. Guided by the observational studies, the model diagnostics and comparisons have focused on predicting the MJO and its modulation of TC activity. Most S2S models have difficulties predicting subseasonal TC activity beyond a seasonal varying climatology, although the skill can be improved by post-process calibration.

The improving availability and skill of subseasonal dynamical models has led to a surge in the number of operational subseasonal forecasts of TCs over the past four years. These forecasts are produced by both dynamical models and statistical methods. Given the increasing skill of these forecasts and the ever-present demand for them, we are very optimistic that these improvements will continue in the coming years.

Appendix A – Acronyms:

AEW	African Easterly Wave
ABY	ACE by Year
ACCESS-S	Australian Community Climate Earth-System Simulator–Seasonal
ACCESS-GE2	Australian Community Climate Earth-System Simulator–Global Ensemble version 2
ACE	Accumulated Cyclone Energy
ATL	Atlantic
AUS	Australia
BoB	Bay of Bengal
BoM	Australian Bureau of Meteorology
BSISO	Boreal Summer Intraseasonal Oscillation
BSS	Brier Skill Score

554	CAM6	Community Atmospheric Model version 6
555	CESM2	Community Earth System Model version 2
556	CFS	Climate Forecast System
557	CMA	China Meteorological Agency
558	CNR-ISAC	Institute for Atmospheric Sciences and Climate, Italy
559	CNRM	National Center for Meteorological Research, Météo-France
560	CPC	Climate Prediction Center
561	CSU	Colorado State University
562	DOD	Department of Defense
563	ECCC	Environment and Climate Change Canada
564	ECEPS	ECMWF Ensemble Prediction System
565	ECMWF	European Center for Medium-range Weather Forecasts
566	ENP	Eastern North Pacific
567	ENSO	El Niño–Southern Oscillation
568	ERW	Equatorial Rossby Waves
569	ESPC	Earth System Prediction Capability
570	GEFSv12	Global Ensemble Forecast System version 12
571	GEOS-S2S-2	Goddard Earth Observing System Subseasonal-to-Seasonal Prediction
572		System v2
573	GFDL	Geophysical Fluid Dynamics Laboratory
574	GloSea5	Global Seasonal forecast system
575	GMAO	Global Modeling and Assimilation Office
576	GPI	Genesis Potential Index

577	GTH	Global Tropical Hazards and Benefits Outlook
578	HiRAM	High Resolution Atmospheric Model
579	HMCR	Hydro-Meteorological Centre of Russia
580	HSS	Heidke Skill Score
581	IFS	Integrated Forecasting System
582	JAMSTEC	Japan Agency for Marine-Earth Science and Technology
583	JMA	Japan Meteorological Agency
584	JTWC	Joint Typhoon Warning Center
585	KMA	Korea Meteorological Agency
586	KW	Kelvin Waves
587	MDR	Main Development Region
588	MetFr	Météo-France
589	MJO	Madden–Julian Oscillation
590	MRG	Mixed Rossby–Gravity Waves
591	MRGTD	Mixed Rossby–Gravity Waves and Tropical Depressions
592	NAO	North Atlantic Oscillation
593	NCEP	National Centers for Environmental Prediction
594	NHC	National Hurricane Center
595	NI	North Indian Ocean
596	NOAA	National Oceanic and Atmospheric Administration
597	NWP	Numerical Weather Prediction
598	OMI	OLR-only MJO Index
599	PC	Principal Component

600	QBWO	Quasi Bi-weekly Oscillation
601	RH	Relative Humidity
602	RPSS	Ranked Probability Skill Score
603	RWB	Rossby Wave Breaking
604	S2S	Subseasonal-to-seasonal
605	SEDS	Symmetric Extreme Dependency Score
606	SIN	South Indian Ocean
607	SPC	Southern Pacific Ocean
608	SPEAR	Seamless System for Prediction and Earth System Research
609	SST	Sea Surface Temperature
610	SubX	Subseasonal Experiment
611	T2F	Time-to-Formation
612	T2H	Time-to-Hurricane
613	TDF	Track Density Function
614	TC	Tropical Cyclone
615	TEHU	Time to Ending Hurricane
616	TETS	Time to Ending Tropical Storm
617	TS	Tropical Storm
618	TUTT	Tropical Upper Tropospheric Trough
619	UKMO	U.K. Met Office
620	WACCM6	Whole Atmosphere Community Climate Model version 6
621	WMO	World Meteorological Organization
622	WNP	Western North Pacific

623 WS Weather Squadron

624

625 *Acknowledgments.* Schreck was supported by NOAA through the Cooperative Institute
626 for Satellite Earth System Studies under Cooperative Agreement NA19NES4320002.
627 Janiga acknowledges the support of the Chief of Naval Research through the NRL Base
628 Program PE 62435N. Camargo and Lee acknowledge support from the NASA MAP
629 program (80NSSC21K1495). Camargo also acknowledges support from NOAA
630 (NA22OAR4310610) and the Vetlesen Foundation. Wang was supported by the National
631 Science Foundation under Grant No. 2116804

632

References

Barton, N., and Coauthors, 2020: The Navy's Earth System Prediction Capability: A New Global Coupled Atmosphere-Ocean-Sea Ice Prediction System Designed for Daily to Subseasonal Forecasting. *Earth and Space Science*, **8**, e2020EA001199, https://doi.org/10.1029/2020EA001199.

Bell, G. D., and Coauthors, 2000: Climate Assessment for 1999. *Bull. Amer. Meteor. Soc.,* **81,** 1328, https://doi.org/10.1175/1520-0477(2000)81[s1:CAF]2.0.CO;2.

BoM, 2020: *Bureau of Meteorology ACCESS-S Multi-Week Tropical Cyclone Guidance: Extended Skill*. http://access-s.clide.cloud/files/guidance_documents/About_weekly_ACCESS-S_TC_forecasts_extended_skill.pdf (Accessed September 22, 2022).

Camargo, S. J., and S. E. Zebiak, 2002: Improving the Detection and Tracking of Tropical Cyclones in Atmospheric General Circulation Models. *Weather and Forecasting*, **17**, 1152–1162, https://doi.org/10.1175/1520-0434(2002)017<1152:ITDATO>2.0.CO;2.

Camargo, S. J., and Coauthors, 2019: Tropical Cyclone Prediction on Subseasonal Time-Scales. *Tropical Cyclone Research and Review*, **8**, 16, https://doi.org/10.6057/2019TCRR03.04.

Camargo, S. J., F. Vitart, C.-Y. Lee, and M. K. Tippett, 2021: Skill, Predictability, and Cluster Analysis of Atlantic Tropical Storms and Hurricanes in the ECMWF Monthly Forecasts. *Monthly Weather Review*, **149**, 3781–3802, https://doi.org/10.1175/MWR-D-21-0075.1.

Camp, J., and Coauthors, 2018: Skilful multiweek tropical cyclone prediction in ACCESS-S1 and the role of the MJO. *Quarterly Journal of the Royal Meteorological Society*, **144**, 1337–1351, https://doi.org/10.1002/qj.3260.

Camp, J, Gregpry P, Marshall AG, Wheeler MC. (2023a) Multi-week tropical cyclone prediction for the Southern Hemisphere in ACCESS-S2: maintaining operational skill and continuity of service. In revision.

Camp, J, Gregpry P, Marshall AG, Wheeler MC. (2023b) Skilful multi-week predictions of tropical cyclone frequency in the Northern Hemisphere using ACCESS-S2. In revision.

Chang, C.-C., and Z. Wang, 2018: Relative Impacts of Local and Remote Forcing on Tropical Cyclone Frequency in Numerical Model Simulations. *Geophysical Research Letters*, **45**, 7843–7850, https://doi.org/10.1029/2018GL078606.

Chu, J.-H., C. R. Sampson, A. S. Levine, and E. Fukada, 2002: The joint typhoon warning center tropical cyclone best-tracks, 1945–2000. *Naval Research Laboratory, Reference Number NRL/MR/7540-02-16*, 22.

Domeisen, D. I. V., and Coauthors, 2022: Advances in the Subseasonal Prediction of Extreme Events: Relevant Case Studies across the Globe. *Bulletin of the American Meteorological Society*, **103**, E1473–E1501, https://doi.org/10.1175/BAMS-D-20-0221.1.

van den Dool, H., E. Becker, L.-C. Chen, and Q. Zhang, 2017: The Probability Anomaly Correlation and Calibration of Probabilistic Forecasts. *Weather and Forecasting*, **32**, 199–206, https://doi.org/10.1175/WAF-D-16-0115.1.

677 Elsberry, R. L., H.-C. Tsai, C. Capalbo, W.-C. Chin, and T. P. Marchok, 2022:
678 Opportunity for Tropical Cyclone Lifecycle Predictions from Pre-Formation to
679 Ending Stage: Eastern North Pacific 2021 Season. *Atmosphere*, **13**, 1008,
680 https://doi.org/10.3390/atmos13071008.
681 Fowler, M. D., and M. S. Pritchard, 2020: Regional MJO Modulation of Northwest
682 Pacific Tropical Cyclones Driven by Multiple Transient Controls. *Geophysical*
683 *Research Letters*, **47**, e2020GL087148, https://doi.org/10.1029/2020GL087148.
684 Gao, K., J. Chen, L. Harris, Y. Sun, and S. Lin, 2019: Skillful Prediction of Monthly
685 Major Hurricane Activity in the North Atlantic with Two-way Nesting. *Geophys.*
686 *Res. Lett.*, **46**, 9222–9230, https://doi.org/10.1029/2019GL083526.
687 Gregory, P., F. Vitart, R. Rivett, A. Brown, and Y. Kuleshov, 2020: Subseasonal
688 Forecasts of Tropical Cyclones in the Southern Hemisphere Using a Dynamical
689 Multimodel Ensemble. *Weather and Forecasting*, **35**, 1817–1829,
690 https://doi.org/10.1175/WAF-D-20-0050.1.
691 Gregory, P. A., J. Camp, K. Bigelow, and A. Brown, 2019: Sub-seasonal predictability of
692 the 2017–2018 Southern Hemisphere tropical cyclone season. *Atmospheric*
693 *Science Letters*, **20**, e886, https://doi.org/10.1002/asl.886.
694 Hansen, K. A., S. J. Majumdar, and B. P. Kirtman, 2020: Identifying Subseasonal
695 Variability Relevant to Atlantic Tropical Cyclone Activity. *Weather and*
696 *Forecasting*, **35**, 2001–2024, https://doi.org/10.1175/WAF-D-19-0260.1.
697 ——, ——, ——, and M. A. Janiga, 2022: Testing Vertical Wind Shear and Nonlinear
698 MJO–ENSO Interactions as Predictors for Subseasonal Atlantic Tropical Cyclone
699 Forecasts. *Weather and Forecasting*, **37**, 267–281, https://doi.org/10.1175/WAF-
700 D-21-0107.1.
701 Hudson et. al., D., 2017: ACCESS-S1 The new Bureau of Meteorology multi-week to
702 seasonal prediction system. *JSHESS*, **67**, 132–159,
703 https://doi.org/10.22499/3.6703.001.
704 Jones, J. J., M. M. Bell, and P. J. Klotzbach, 2020: Tropical and Subtropical North
705 Atlantic Vertical Wind Shear and Seasonal Tropical Cyclone Activity. *Journal of*
706 *Climate*, **33**, 5413–5426, https://doi.org/10.1175/JCLI-D-19-0474.1.
707 ——, ——, ——, and E. A. Barnes, 2022: Wintertime Rossby Wave Breaking
708 Persistence in Extended-Range Seasonal Forecasts of Atlantic Tropical Cyclone
709 Activity. *Journal of Climate*, **35**, 2133–2147, https://doi.org/10.1175/JCLI-D-21-
710 0213.1.
711 Kiladis, G. N., J. Dias, K. H. Straub, M. C. Wheeler, S. N. Tulich, K. Kikuchi, K. M.
712 Weickmann, and M. J. Ventrice, 2014: A Comparison of OLR and Circulation-
713 Based Indices for Tracking the MJO. *Mon. Wea. Rev.*, **142**, 1697–1715,
714 https://doi.org/10.1175/MWR-D-13-00301.1.
715 Kolstad, E. W., 2021: Prediction and precursors of Idai and 38 other tropical cyclones
716 and storms in the Mozambique Channel. *Quarterly Journal of the Royal*
717 *Meteorological Society*, **147**, 45–57, https://doi.org/10.1002/qj.3903.
718 Landu, K., R. Goyal, and B. S. Keshav, 2020: Role of multiple equatorial waves on
719 cyclogenesis over Bay of Bengal. *Clim Dyn*, **54**, 2287–2296,
720 https://doi.org/10.1007/s00382-019-05112-5.

721 Lee, C.-Y., S. J. Camargo, F. Vitart, A. H. Sobel, and M. K. Tippett, 2018: Subseasonal
722 Tropical Cyclone Genesis Prediction and MJO in the S2S Dataset. *Wea.*
723 *Forecasting*, **33**, 967–988, https://doi.org/10.1175/WAF-D-17-0165.1.
724 ——, ——, ——, ——, J. Camp, S. Wang, M. K. Tippett, and Q. Yang, 2020:
725 Subseasonal Predictions of Tropical Cyclone Occurrence and ACE in the S2S
726 Dataset. *Weather and Forecasting*, **35**, 921–938, https://doi.org/10.1175/WAF-D-
727 19-0217.1.
728 Li, W., Z. Wang, G. Zhang, M. S. Peng, S. G. Benjamin, and M. Zhao, 2018:
729 Subseasonal Variability of Rossby Wave Breaking and Impacts on Tropical
730 Cyclones during the North Atlantic Warm Season. *Journal of Climate*, **31**, 9679–
731 9695, https://doi.org/10.1175/JCLI-D-17-0880.1.
732 Ling, Z., Y. Wang, G. Wang, and H. He, 2020: Impact of Intraseasonal Oscillations on
733 the Activity of Tropical Cyclones in Summer Over the South China Sea: Nonlocal
734 Tropical Cyclones. *Frontiers in Earth Science*, **8**,
735 https://doi.org/10.3389/feart.2020.609776.
736 Long, L. N., N. Novella, and J. Gottschalck, 2020: The New Probabilistic Global Tropics
737 Hazards Outlook at CPC: Weeks 2 and 3. *Science and Technology Infusion*
738 *Climate Bulletin*, 45th NOAA Annual Climate Diagnostics and Prediction
739 Workshop, Virtual Online, NOAA's National Weather Service.
740 MacLachlan, C., and Coauthors, 2015: Global Seasonal forecast system version 5
741 (GloSea5): a high-resolution seasonal forecast system. *Quarterly Journal of the*
742 *Royal Meteorological Society*, **141**, 1072–1084, https://doi.org/10.1002/qj.2396.
743 Maier-Gerber, M., A. H. Fink, M. Riemer, E. Schoemer, C. Fischer, and B. Schulz, 2021:
744 Statistical–Dynamical Forecasting of Subseasonal North Atlantic Tropical
745 Cyclone Occurrence. *Weather and Forecasting*, **36**, 2127–2142,
746 https://doi.org/10.1175/WAF-D-21-0020.1.
747 Molod, A., and Coauthors, 2020: GEOS-S2S Version 2: The GMAO High-Resolution
748 Coupled Model and Assimilation System for Seasonal Prediction. *Journal of*
749 *Geophysical Research: Atmospheres*, **125**, e2019JD031767,
750 https://doi.org/10.1029/2019JD031767.
751 Nakano, M., F. Vitart, and K. Kikuchi, 2021: Impact of the Boreal Summer Intraseasonal
752 Oscillation on Typhoon Tracks in the Western North Pacific and the Prediction
753 Skill of the ECMWF Model. *Geophysical Research Letters*, **48**, e2020GL091505,
754 https://doi.org/10.1029/2020GL091505.
755 Papin, P. P., 2017: Variations in potential vorticity streamer activity: Development
756 pathways, environmental impacts, and links to tropical cyclone activity in the
757 North Atlantic basin. University at Albany, State University of New York, 225
758 pp.
759 ——, L. F. Bosart, and R. D. Torn, 2020: A Feature-Based Approach to Classifying
760 Summertime Potential Vorticity Streamers Linked to Rossby Wave Breaking in
761 the North Atlantic Basin. *Journal of Climate*, **33**, 5953–5969,
762 https://doi.org/10.1175/JCLI-D-19-0812.1.
763 Pegion, K., and Coauthors, 2019: The Subseasonal Experiment (SubX): A Multimodel
764 Subseasonal Prediction Experiment. *Bulletin of the American Meteorological*
765 *Society*, **100**, 2043–2060, https://doi.org/10.1175/BAMS-D-18-0270.1.

Postel, G. A., and M. H. Hitchman, 1999: A Climatology of Rossby Wave Breaking along the Subtropical Tropopause. *Journal of the Atmospheric Sciences*, **56**, 359–373, https://doi.org/10.1175/1520-0469(1999)056<0359:ACORWB>2.0.CO;2.

Qian, Y., P.-C. Hsu, H. Murakami, B. Xiang, and L. You, 2020: A Hybrid Dynamical-Statistical Model for Advancing Subseasonal Tropical Cyclone Prediction Over the Western North Pacific. *Geophysical Research Letters*, **47**, e2020GL090095, https://doi.org/10.1029/2020GL090095.

Richter, J. H., and Coauthors, 2022: Subseasonal Earth System Prediction with CESM2. *Weather and Forecasting*, **37**, 797–815, https://doi.org/10.1175/WAF-D-21-0163.1.

Takemura, K., and H. Mukougawa, 2021: Tropical Cyclogenesis Triggered by Rossby Wave Breaking over the Western North Pacific. *SOLA*, **17**, 164–169, https://doi.org/10.2151/sola.2021-029.

Vitart, F., 2017: Madden—Julian Oscillation prediction and teleconnections in the S2S database. *Quarterly Journal of the Royal Meteorological Society*, **143**, 2210–2220, https://doi.org/10.1002/qj.3079.

——, and T. N. Stockdale, 2001: Seasonal Forecasting of Tropical Storms Using Coupled GCM Integrations. *Monthly Weather Review*, **129**, 2521–2537, https://doi.org/10.1175/1520-0493(2001)129<2521:SFOTSU>2.0.CO;2.

Vitart, F., A. Leroy, and M. C. Wheeler, 2010: A Comparison of Dynamical and Statistical Predictions of Weekly Tropical Cyclone Activity in the Southern Hemisphere. *Mon. Wea. Rev.*, **138**, 3671–3682, https://doi.org/10.1175/2010MWR3343.1.

Vitart, F., and Coauthors, 2017: The Subseasonal to Seasonal (S2S) Prediction Project Database. *Bulletin of the American Meteorological Society*, **98**, 163–173, https://doi.org/10.1175/BAMS-D-16-0017.1.

Wang, S., A. H. Sobel, M. K. Tippett, and F. Vitart, 2019: Prediction and predictability of tropical intraseasonal convection: seasonal dependence and the Maritime Continent prediction barrier. *Clim Dyn*, **52**, 6015–6031, https://doi.org/10.1007/s00382-018-4492-9.

Wang, Z., G. Zhang, T. Dunkerton, F.-F. Jin, 2020: Summertime stationary waves integrate tropical and extratropical impacts on tropical cyclone activity. *PNAS,* **117,** 22720-22726, https://doi.org/10.1073/pnas.2010547117.

Wedd, R., and Coauthors, 2022: ACCESS-S2: the upgraded Bureau of Meteorology multi-week to seasonal prediction system. *JSHESS*, **72**, 218–242, https://doi.org/10.1071/ES22026.

World Meteorological Organization (WMO), 2021: *State of the Global Climate 2021 : WMO Provisional report*. WMO, 47 p. pp.

Xiang, B., and Coauthors, 2022a: S2S Prediction in GFDL SPEAR: MJO Diversity and Teleconnections. *Bulletin of the American Meteorological Society*, **103**, E463–E484, https://doi.org/10.1175/BAMS-D-21-0124.1.

——, B. Wang, W. Zhang, L. Harris, T. L. Delworth, G. Zhang, and W. F. Cooke, 2022b: Subseasonal controls of U.S. landfalling tropical cyclones. *npj Clim Atmos Sci*, **5**, 1–9, https://doi.org/10.1038/s41612-022-00289-9.

Zhang, G., Z. Wang, T. J. Dunkerton, M. S. Peng, and G. Magnusdottir, 2016: Extratropical Impacts on Atlantic Tropical Cyclone Activity. *J. Atmos. Sci.*, **73**, 1401–1418, https://doi.org/10.1175/JAS-D-15-0154.1.

——, ——, M. S. Peng, and G. Magnusdottir, 2017: Characteristics and Impacts of Extratropical Rossby Wave Breaking during the Atlantic Hurricane Season. *Journal of Climate*, **30**, 2363–2379, https://doi.org/10.1175/JCLI-D-16-0425.1.

——, and Coauthors, 2021: Seasonal predictability of baroclinic wave activity. *npj Clim Atmos Sci*, **4**, 1–11, https://doi.org/10.1038/s41612-021-00209-3.

Zhao, H., X. Jiang, L. Wu, and P. J. Klotzbach, 2019: Multi-scale interactions of equatorial waves associated with tropical cyclogenesis over the western North Pacific. *Clim Dyn*, **52**, 3023–3038, https://doi.org/10.1007/s00382-018-4307-z.

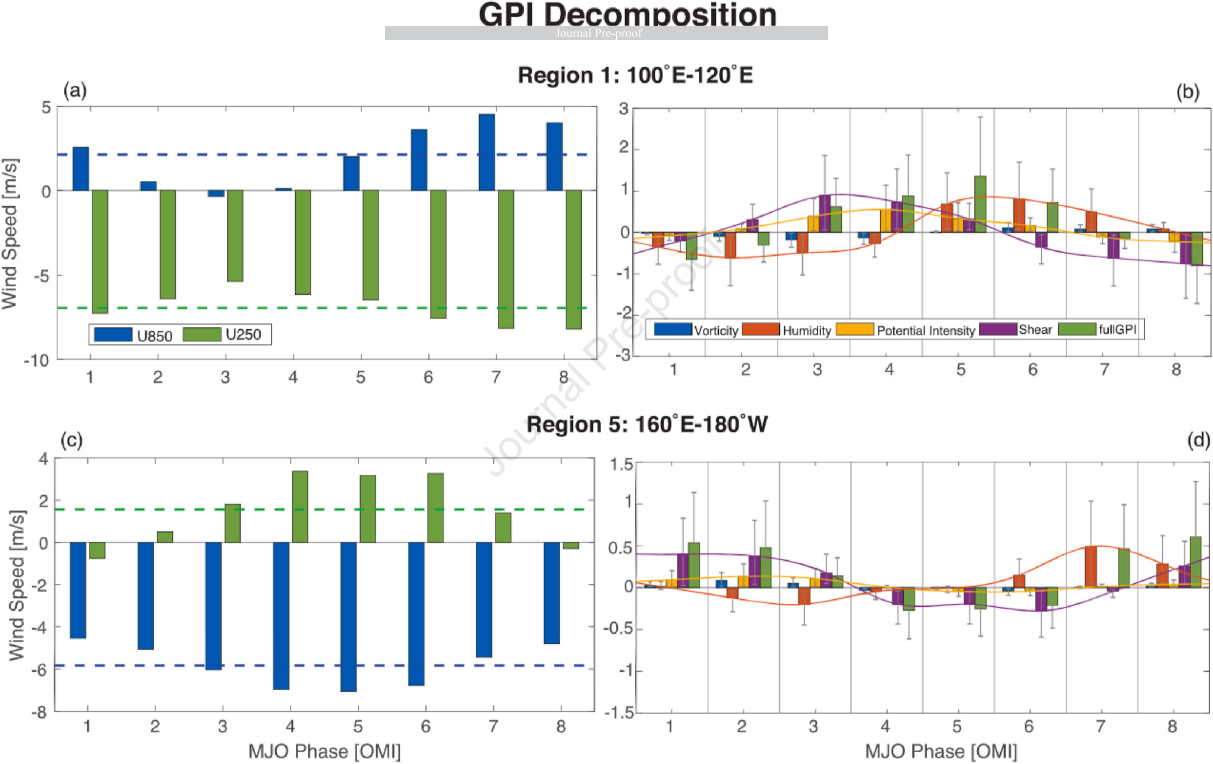

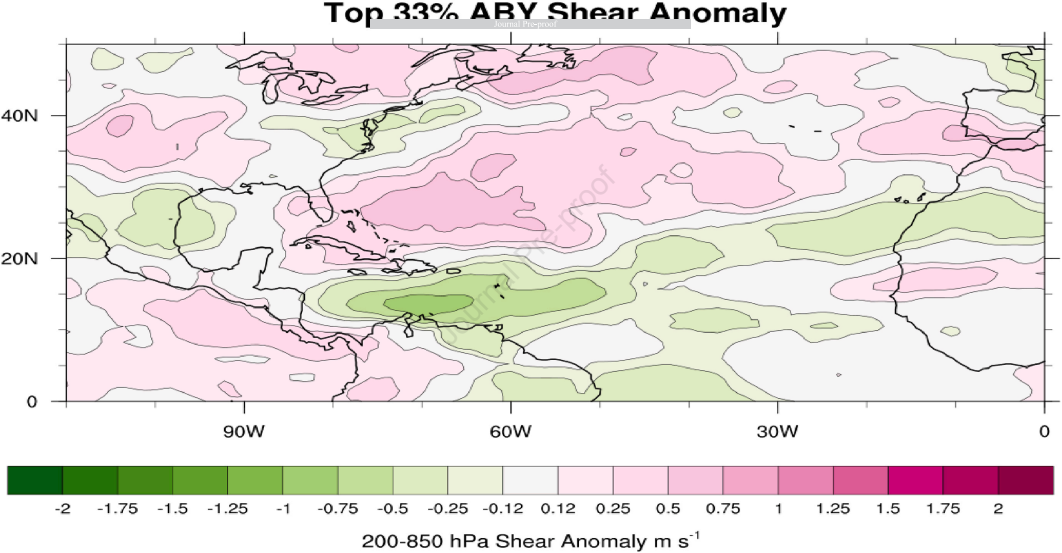
Top 33% ABY Shear Anomaly
40N
20N
0
90W
60W
30W
0
-2
-1.75
-1.5
-1.25
-1
-0.75
-0.5
-0.25
-0.12
0.12
0.25
0.5
0.75
1
1.25
1.5
1.75
2
200-850 hPa Shear Anomaly m s-1

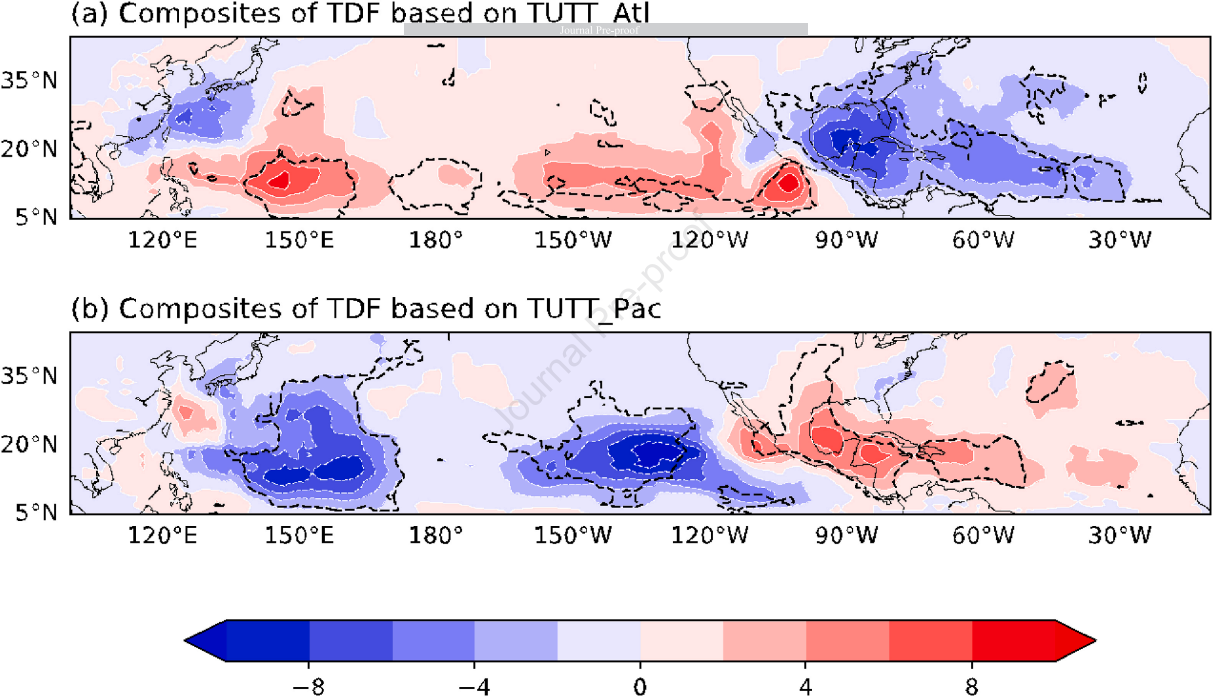
(a) Composites of TDF based on TUTT_Atl
35°N
20°N
5°N
120°E
150°E
180°
150°W
120°W
90°W
60°W
30°W
(b) Composites of TDF based on TUTT_Pac
35°N
20°N
5°N
120°E
150°E
180°
150°W
120°W
90°W
60°W
30°W
−8
−4
0
4
8

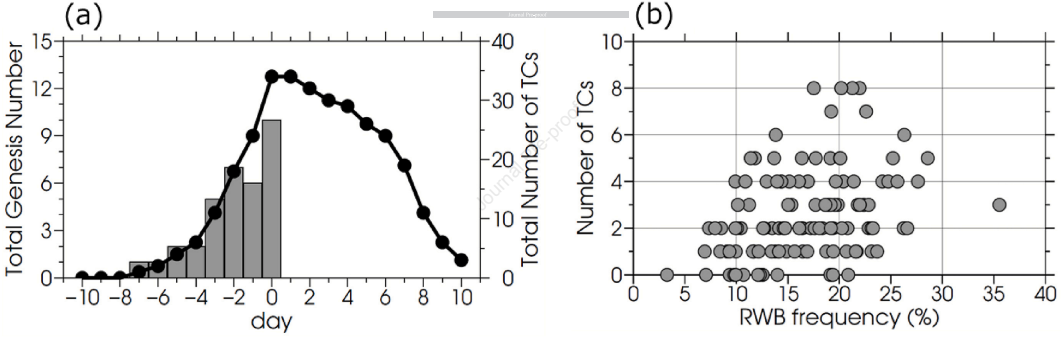
(a)
Total Genesis Number
Total Number of TCs
day
(b)
Number of TCs
RWB frequency (%)

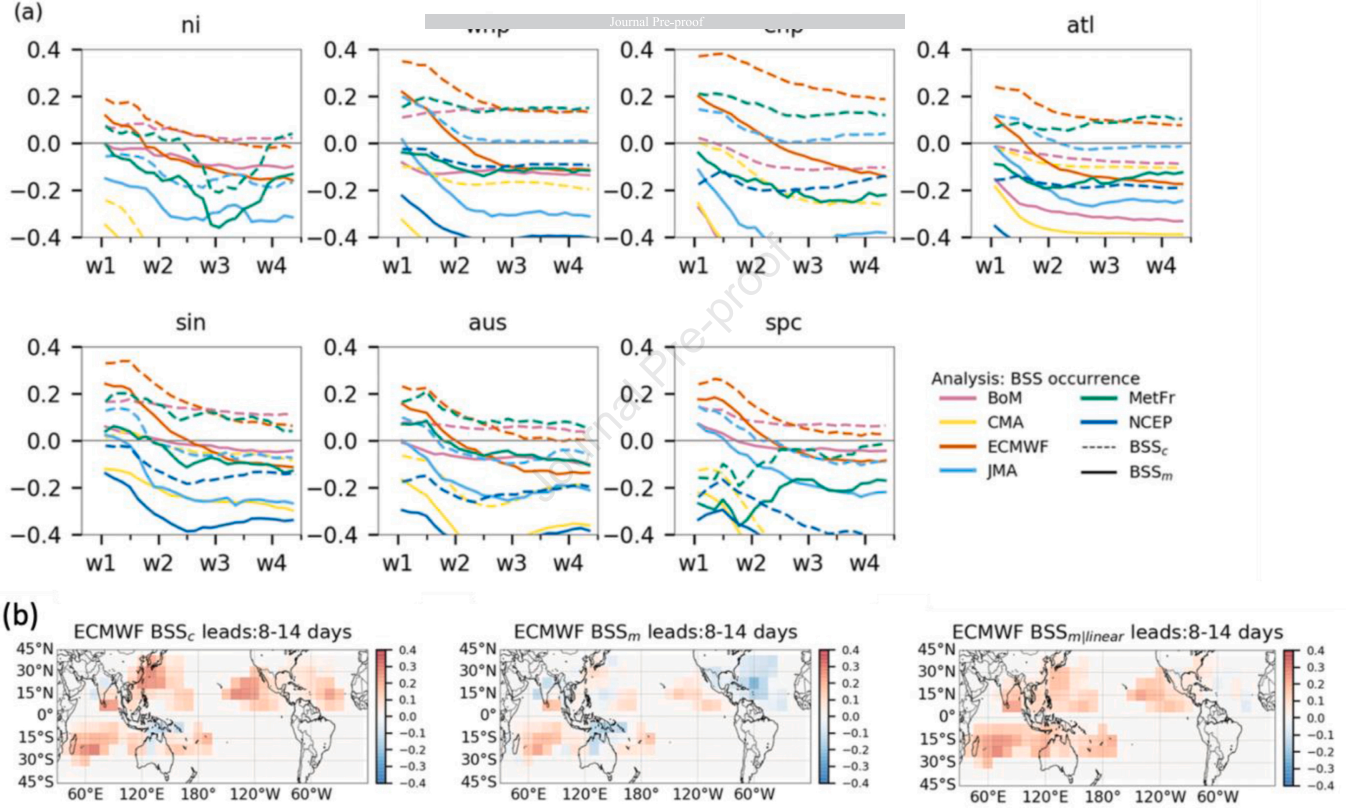

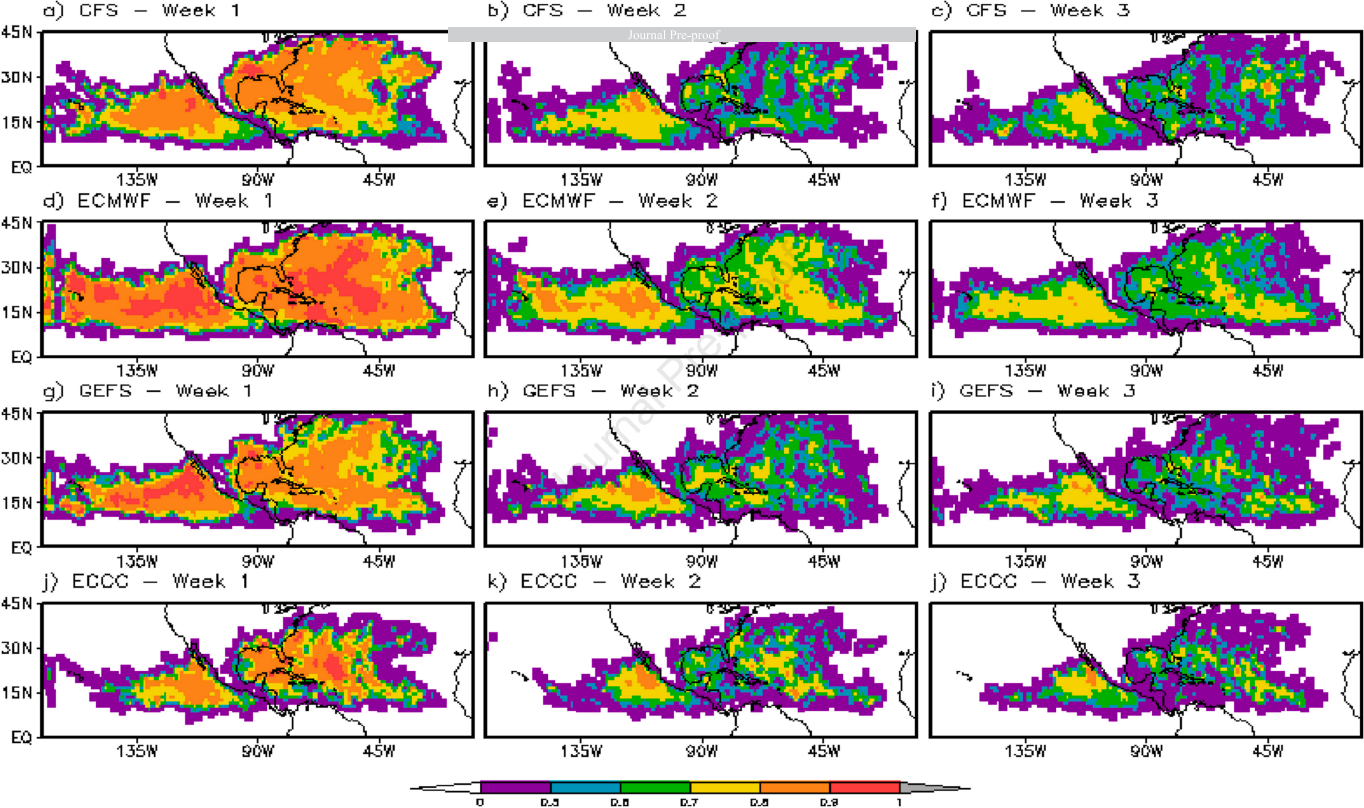

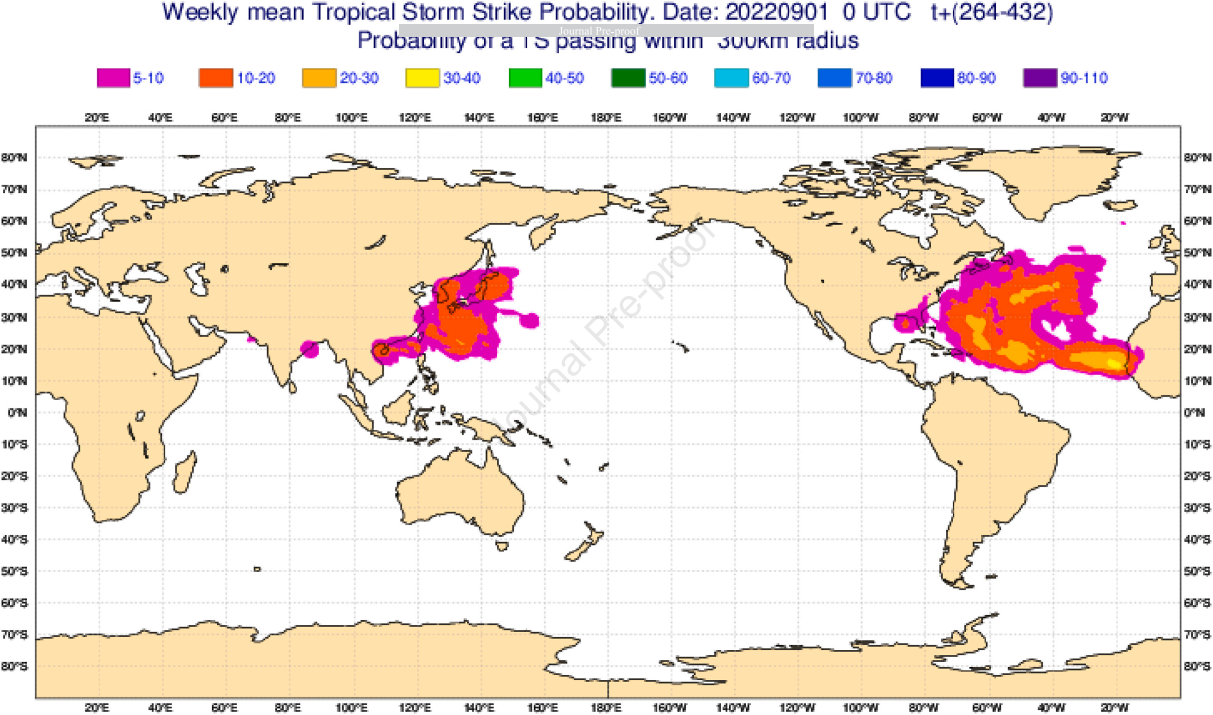
Weekly mean Tropical Storm Strike Probability. Date: 20220901 0 UTC t+(264-432)
Probability of a TS passing within 300km radius
5-10
10-20
20-30
30-40
40-50
50-60
60-70
70-80
80-90
90-110
20°E 40°E 60°E 80°E 100°E 120°E 140°E 160°E 180°E 160°W 140°W 120°W 100°W 80°W 60°W 40°W 20°W
80°N 70°N 60°N 50°N 40°N 30°N 20°N 10°N 0°N 10°S 20°S 30°S 40°S 50°S 60°S 70°S 80°S